Huo *et al. J Transl Med* (2021) 19:183
https://doi.org/10.1186/s12967-021-02846-x

Journal of Translational Medicine

RESEARCH

Open Access

Eleven immune-gene pairs signature associated with TP53 predicting the overall survival of gastric cancer: a retrospective analysis of large sample and multicenter from public database

Junyu Huo[1,2], Liqun Wu[1*] and Yunjin Zang[1]

Abstract

Background: Growing attention have been paid to the relationship between TP53 and tumor immunophenotype, but there are still lacking enough search on the field of gastric cancer (GC).

Materials and methods: We identified differential expressed immune-related genes (DEIRGs) between the TP53-altered GC samples (n = 183) and without TP53-altered GC samples (n = 192) in The Cancer Genome Atlas and paired them. In the TCGA cohort (n = 350), a risk score was determined through univariate and multivariate cox regression and Lasso regression analysis. Patients were divided into two groups, high-risk and low-risk, based on the median risk score. Four independent cohorts (GSE84437,n = 431; GSE62254, n = 300; GSE15459, n = 191; GSE26901, n = 100) from the Gene Expression Omnibus (GEO) database were used to validate the reliability and universal applicability of the model.

Results: The signature contained 11 gene pairs showed good performance in predicting progression-free survival (PFS), disease-free survival (DFS), disease special survival (DSS), and the overall survival (OS) for GC patients in the TCGA cohort. The subgroup analysis showed that the signature was suitable for GC patients with different characteristics. The signature could capable of distinguish GC patients with good prognosis and poor prognosis in all four independent external validation cohorts. The high- and low-risk groups differed significantly in the proportion of several immune cell infiltration, especially for the T cells memory resting, T cells memory activated and follicular helper, and Macrophage M0, which was also related to the prognosis of GC patients.

Conclusion: The present work proposed an innovative system for evaluating the prognosis of gastric cancer. Considering its stability and general applicability, which may become a widely used tool in clinical practice.

Keywords: Gastric cancer, Immune, Gene pairs, Prognostic, Signature

Background

Gastric cancer (GC) is a typical malignant tumor in clinical practice. Its incidence rate and mortality rate were the second highest in the world [1]. Surgery combined with radiotherapy and chemotherapy is the main method for the treatment of GC. However, due to the

*Correspondence: wulq5810@126.com
[1] Liver Disease Center, The Affiliated Hospital of Qingdao University, No. 59 Haier Road, Qingdao 266003, China
Full list of author information is available at the end of the article

© The Author(s) 2021. This article is licensed under a Creative Commons Attribution 4.0 International License, which permits use, sharing, adaptation, distribution and reproduction in any medium or format, as long as you give appropriate credit to the original author(s) and the source, provide a link to the Creative Commons licence, and indicate if changes were made. The images or other third party material in this article are included in the article's Creative Commons licence, unless indicated otherwise in a credit line to the material. If material is not included in the article's Creative Commons licence and your intended use is not permitted by statutory regulation or exceeds the permitted use, you will need to obtain permission directly from the copyright holder. To view a copy of this licence, visit http://creativecommons.org/licenses/by/4.0/. The Creative Commons Public Domain Dedication waiver (http://creativecommons.org/publicdomain/zero/1.0/) applies to the data made available in this article, unless otherwise stated in a credit line to the data.

occult early symptoms of GC, most patients were in the advanced stage when diagnosed, and less than 20% could survive 5 years [2]. With the wide promotion of precision medicine, the research on gene molecular targeted precise therapy has become a hot topic in the field of cancer.

The high mutation rate of TP53 in tumors makes it a very attractive potential therapeutic target [3]. In the cell cycle, normal p53 is activated during DNA damage or hypoxia, which stagnates the cell cycle at G1/S point and carried out DNA repair. If the repair fails, downstream genes were activated to induce apoptosis. Both of these functions help to reduce the possibility of tumorigenesis [4]. A study of 3281 tumors involving 12 tumor types found that the average mutation frequency of TP53 was about 42% [5]. A report from 10,225 patients with 32 different cancers from the Cancer Genome Atlas (TCGA) showed that TP53 mutations were more frequent in cancer patients with lower survival rates among all cancer types studied [3]. These data indicated the crucial role of the TP53 mutation in the occurrence and development of malignant tumor.

TP53 can be used for ultra-early screening of GC, and can be used to monitor postoperative recurrence of gastric cancer by monitoring free DNA mutations, and predicting the efficacy of paclitaxel combined with capecitabine in the treatment of advanced GC [6, 7]. Interestingly, some recent studies have shown that different immune responses are associated with TP53 mutation status [8–11]. Immunotherapy, as a new treatment for GC, has great potential in clinical application [12]. Although there are few studies on the relationship between TP53 mutation and the efficacy of immunotherapy in GC, there was increasing evidence suggested that the TP53 mutation can affect the immunophenotype of GC [13–15]. Although the mechanism of TP53 mutation affects the immunophenotypic regulation of GC remains unclear, considering the important role of TP53 in maintaining genomic stability, the change of immune genome expression pattern mediated by TP53 mutation may affect the immunophenotype of GC and lead to different clinical outcomes.

In our work, we paired the differential immune-related genes associated with TP53 mutation and studied the effect of this combination on the overall prognosis of GC. We developed a prognosis model contained 11 immune gene pairs based on TCGA datasets and used four independent cohorts from GEO database to validate its prognostic value for GC. This large sample, multicenter analysis may provide an important basis for the comprehensive management of GC.

Materials and methods

Data collection

In terms of the 375 GC tissues, their RNA-sequencing profile was obtained from The Cancer Genome Atlas (TCGA, https://portal.gdc.cancer.gov/). The complete prognostic information of 350 GC patients was available in the TCGA database. The TP53- alterated sample list was acquired from the cBioPortal (https://www.cbioportal.org/). The gene expression files and corresponding clinical data of four independent cohorts (GSE84437, n = 431; GSE62254, n = 300; GSE15459, n = 191; GSE26901, n = 100) were downloaded from the Gene Expression Omnibus (GEO) database (https:// www.ncbi.nlm.nih.gov/geo/). The downloaded profiles were all complied with the TCGA and GEO data access rules. The detailed clinical information of the above five datasets were displayed in Table 1. The data utilized in this work were obtained from public databases, so the approval from the local ethics committee was not needed.

Identification of differential expressed immune-related genes (DEIRGs)

The list of genes related to immune came from the ImmPort database (https://immport.niaid.nih.gov) (Additional file 1) and we extracted them from TCGA datasets. The "edgeR" R package was used to identifying DEIRGs in TP53-altered GC samples (n = 183) and without TP53-altered GC samples (n = 192). A false discovery rate (FDR) of < 0.05 was considered significant. The R package "cluster profile" was applied for DEIRGs annotation (Kyoto Encyclopedia of Genes and Genomes).

Construction of immune gene pairs

We paired the DEIRGs. In each immune gene pair (IGP), if the former gene presented a higher expression relative to the latter one, the value was defined to 1. On the contrary, if the expression level of the former gene was lower compared to the latter one, the value was defined to 0. The IGPs with proportion of "0" or "1" less than 20% were excluded. Since the IGPs were generated by a pairwise comparison and were entirely based on the gene expression in the same patient, the gene expression profiles of different platforms did not need to be normalized.

Construction and validation of the immune gene pairs prognostic model

The prognostic related immune gene pairs (PRIGPs) were identified by the univariate Cox regression analysis first [16]. P < 0.001 was considered to be significant. Next, the scope of PRIGPs was reduced by the least absolute shrinkage and selection operator (LASSO) algorithm, as well as penalty parameter tuning based on tenfold cross-validation [17]. Then we input the IGPs

with nonzero regression coefficients to the multivariate cox regression analysis. After that, multivariate Cox regression coefficients were calculated to establish a risk score. Patients were divided into low-risk and high-risk

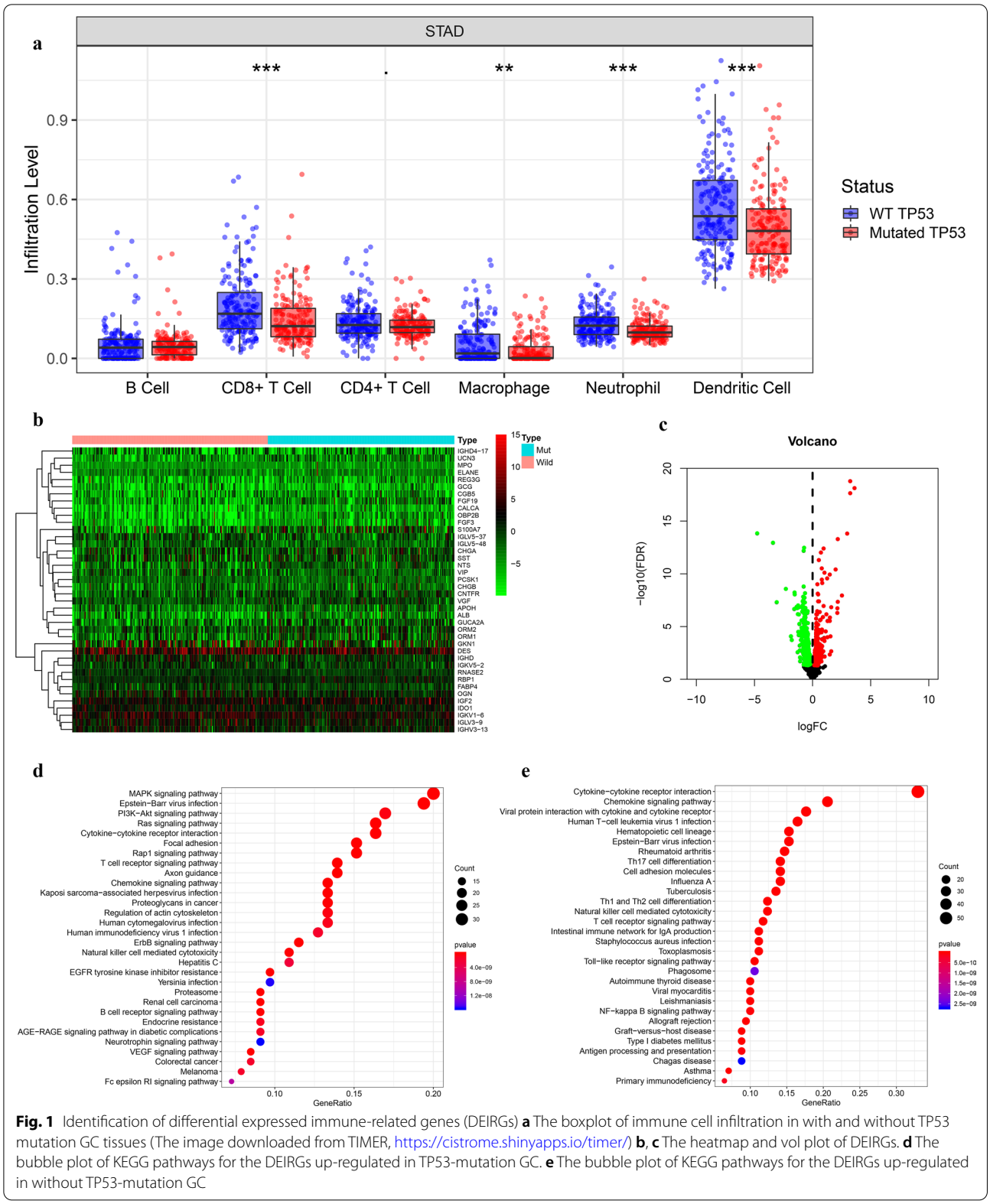

Fig. 1 Identification of differential expressed immune-related genes (DEIRGs) **a** The boxplot of immune cell infiltration in with and without TP53 mutation GC tissues (The image downloaded from TIMER, https://cistrome.shinyapps.io/timer/) **b**, **c** The heatmap and vol plot of DEIRGs. **d** The bubble plot of KEGG pathways for the DEIRGs up-regulated in TP53-mutation GC. **e** The bubble plot of KEGG pathways for the DEIRGs up-regulated in without TP53-mutation GC

groups based on the median risk score of the TCGA cohort (n = 350). LASSO regression analysis was carried out with the "glmnet" R package. R package "survminer" and "survivalROC" were employed to obtain the receiver operating characteristic (ROC) curve and the Kaplan–Meier survival curve. The prognostic model's independent prognostic value was evaluated through the univariate and multivariate Cox regression analysis. The predictive capability and applicability of the prognostic model were verified based on four independent external validation cohorts including GSE84437 (n = 431), GSE62254 (n = 300), GSE15459 (n = 191) and GSE26901(n = 100).

Immune infiltration analysis between different risk groups

The CIBERSORT algorithm was used for quantifying 22 kinds of immune cell infiltration proportions of all the included 1372 GC samples (TCGA, n = 350; GSE84437, n = 431; GSE62254, n = 300; GSE15459, n = 191; GSE26901, n = 100) [18–20]. We used $p < 0.05$ as the threshold to judge the accuracy of prediction of immune cell infiltration, the samples with $p < 0.05$ could be used for subsequent analysis.

Results

Identification of DEIRGs associated with TP53

Tumor IMmune Estimation Resource (TIMER) algorithm could predict the composition of infiltrating immune cells in each tumor sample based on the gene expression profile data of tumor samples [21, 22]. We used the TIMER algorithm to estimate the abundances of six immune infiltrates (B cells, CD4 + T cells, CD8 + T cells, Neutrophils, Macrophages, and Dendritic cells) in GC samples, and found that the infiltration level of CD8 T cells, dendritic cells, neutrophils and Macrophages exhibited obviously difference in the mutated-TP53 and WT-TP53 GC tissues (Fig. 1a). Next, we identified 512 DEIRGs in TP53-altered and without TP53-altered GC samples. Among them, 216 genes were up-regulated in 183 TP53-altered GC samples, and 296 genes were up-regulated in 192 without TP53-altered GC samples (Fig. 1b, c). The KEGG pathway enriched by up-regulated immune genes in GC samples with TP53 mutation and without TP53 mutation was also different (Fig. 1d, e). These results confirmed the hypothesis of the immunophenotype of GC may affected by the TP53 mutation. The workflow of our paper as shown in Fig. 2.

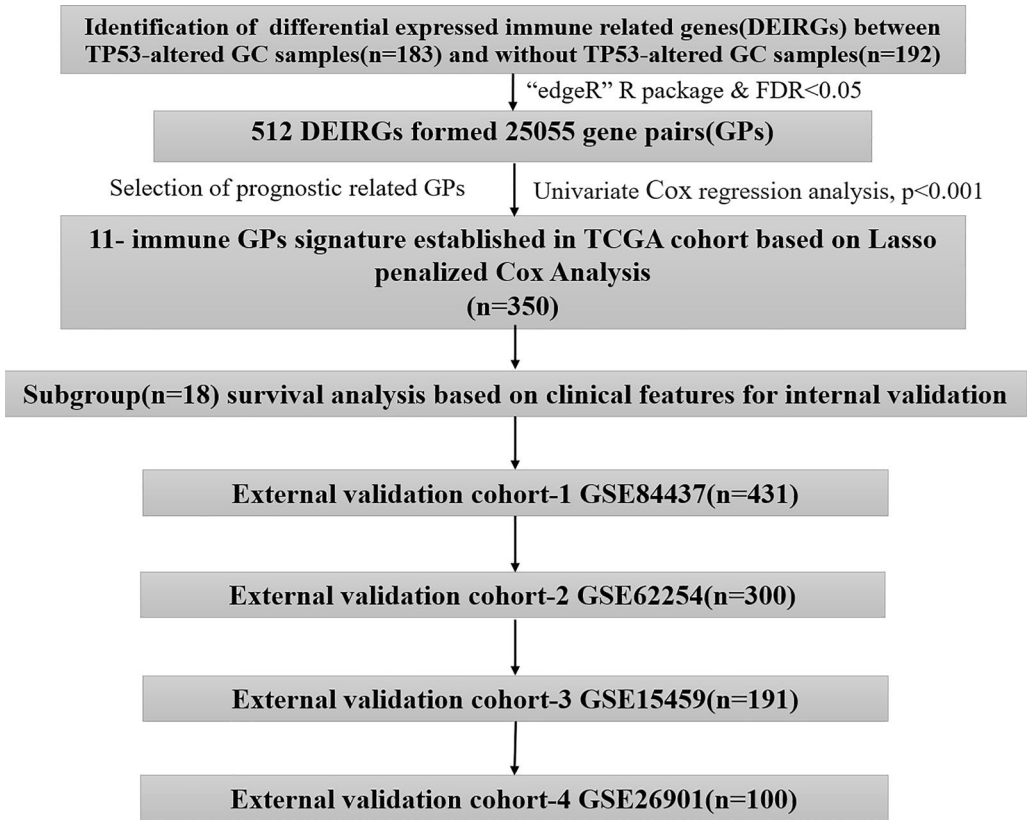

Fig. 2 The workflow chart of this study

Construction of the immune gene pairs prognostic model in TCGA cohort

After a pairwise comparison, 512 DEIRGs formed 25,055 gene pairs (GPs), 105,761 GPs were excluded from 130.816 GPs because the proportion of "0" or "1" was less than 20%. The univariate Cox regression analysis revealed the significant correlation of 42 GPs with overall survival ($p < 0.001$) (Fig. 3a). The 42 GPs were further reduced by Lasso penalty Cox regression analysis, among which 21 GPs were repeated more than 900times after 1000 times tenfold cross-validation (Fig. 3b). Finally, a risk score was constructed after the selection of 11 GPs by step-by-step multivariate Cox regression (Fig. 3c). The median risk score-0.948 was used to divide the GC patients into two groups, low-risk and high-risk. The specific calculation formula of risk score as shown in Table 2.

Prognostic assessment of the model in the TCGA cohort

Four prognostic indicators (PFS, progression-free survival; DFS, disease-free survival; DSS, disease special survival; OS, overall survival) were used to evaluate the prognostic value of the model for GC. As shown in Fig. 4, the high-risk group obtained lower values of OS, DSS, DFS, and PFS than the low-risk group (Fig. 4a–d). The area under curve (AUC) values for the model predicting OS at 1, 3 and 5 years were 0.754, 0.770 and 0.823 respectively. The AUC values for the model predicting PFS at 1,3 and 5 years were 0.701,0.744 and 0.716 respectively. The model predicting DSS obtained a result of 0.775,0.773 and 0.810 correspondingly. The model predicting DFS got a result of 0.784,0.792 and 0.705 (Fig. 4a–d). These results demonstrated the good performance of this prognostic model.

Internal validation of the prognostic model in the TCGA cohort

The clinical features were used to divide TCGA-GC patients into 18 subgroups. High-risk patients had significantly lower OS than low-risk patients in each subgroup (Fig. 5a–g). By observing the time-dependent ROC curves, we found that the AUC value of risk score was the highest in predicting OS of patients with GC at 1, 3 and 5 years, which showed that the prediction accuracy of risk score is higher than the existing TNM staging prognosis evaluation system (Fig. 6a–c). The Decision Curve Analysis (DCA) [23] were also confirmed that the risk score could bring the greatest clinical net benefit to patients (Fig. 6d). The general applicability of the prognostic model was preliminarily confirmed.

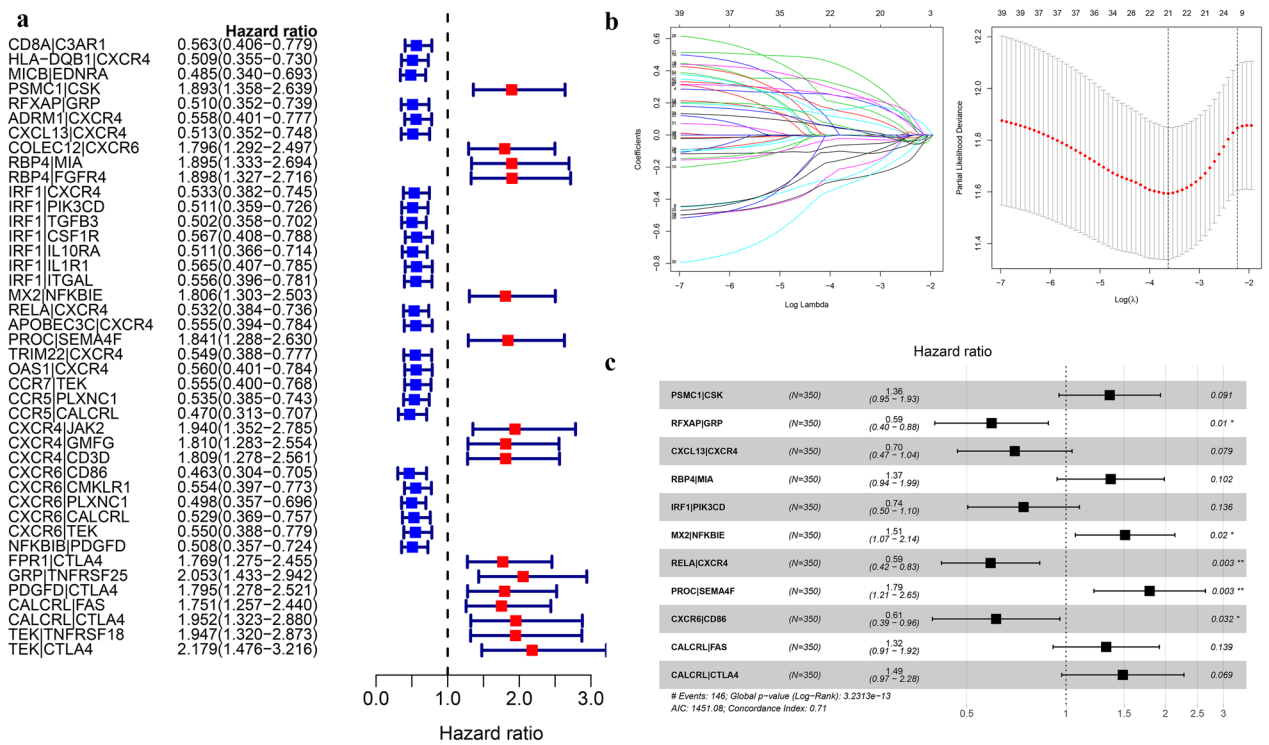

Fig. 3 The building process of the 11 immune gene pairs prognostic signature (**a**). The forrest plot of the univariate Cox analysis. **b** Lasso regression analysis. **c** Multivariate Cox regression analysis

Table 1 The clinical data of the 5 independent cohorts

	TCGA (n = 350)	GSE84437(n = 431)	GSE62254(n = 300)	GSE15459(n = 191)	GSE26901(n = 100)
Survival status					
Alive	204	224	148	96	45
Dead	146	207	152	95	55
Age					
> 65	189	150	97	108	23
< = 65	158	283	136	83	77
Gender					
Female	123	137	74	67	39
Male	224	296	159	124	61
Grade					
G1–2	134				
G3	207				
Stage T					
T1–2	90	49			
T3	161	92			
T4	95	292			
Stage N					
N0	103	80			
N1	93	188			
N2	72	132			
N3	71	33			
Stage M					
M0	312				
M1	23				
Stage TNM					
I–II	156		139	60	52
III	145		75	72	33
IV	35		19	59	15
Laurenclassificatio n					
Diffuse		102	122	75	11
Intestinal		119	105	98	74
Mixed		10	6	18	5
Perineural Invasion					
Yes			86		
No			147		
Lymphovascular					
Yes			171		
No			62		
Subtype					
Invasive				51	
Metabolic				40	
Proliferative				69	
Unstable				31	
Subgroup					
MP					39
EP					61
Adjuvant.chem					
Yes					37
No					63

Table 1 (continued)

	TCGA (n = 350)	GSE84437(n = 431)	GSE62254(n = 300)	GSE15459(n = 191)	GSE26901(n = 100)
Location					
Antrum					51
Body					34
Entire					4
Fundus					11

Table 2 The list of gene pairs and corresponding coefficient

Gene pairs	Coef
PSMC1|CSK	0.304948
RFXAP|GRP	− 0.51969
CXCL13|CXCR4	− 0.35784
RBP4|MIA	0.311735
IRF1|PIK3CD	− 0.29637
MX2|NFKBIE	0.412191
RELA|CXCR4	− 0.52646
PROC|SEMA4F	0.583495
CXCR6|CD86	− 0.48794
CALCRL|FAS	0.280125
CALCRL|CTLA4	0.396375

External validation of the prognostic model in four independent cohorts

The risk score of GC patients in each independent cohort was calculated. These patients were classified into two groups, high-risk and low-risk, on the basis of the unified cutoff-0.948. All high-risk patients had significantly lower OS values than low-risk patients in each independent cohort (Fig. 7a, d, g, j). In the GSE84437 cohort (n = 431), the area under curve (AUC) values for the model predicting OS at 1, 3 and 5 years were 0.583,0.616 and 0.643 respectively (Fig. 7b). In the GSE62254 cohort (n = 300), the results were 0.660, 0.675 and 0.675 correspondingly (Fig. 7e). The results of the GSE15459 cohort (n = 191) were 0.628,0.635 and 0.641 (Fig. 7h). The results of the GSE26901 cohort (n = 100) were 0.714,0.707 and 0.615 (Fig. 7k). The risk of death increased with the increase of risk score (Fig. 7c, f, i, l). We pooled four independent validation cohort (a total of 1022 patients) for analysis, and found that the survival difference between high-risk group and low-risk group was still significant (Fig. 8a, b). The OS of high-risk patients in each subgroup divided by clinical traits were also significantly lower than that in the low-risk group (Fig. 8c). These results further confirmed the stability and general applicability of the our established prognostic model.

The prognostic model as an independent prognostic indicator

We included the risk score and other clinical factors into the univariate and multivariate Cox regression analysis, as the results suggested that the risk score was an independent prognostic indicator in the TCGA, GSE84437, and GSE62254 cohort (Fig. 9a–c). However, in the GSE15459 and GSE26901 cohorts, the risk score could be considered as an independent prognostic risk factor for GC only when TNM staging was excluded from multivariate Cox regression analysis (Fig. 9d, e).

The difference of immune cell infiltration between two groups

With $p < 0.05$ as the threshold, 335 samples with p value greater than 0.05 as predictive inaccurate samples were excluded. We integrated the immune infiltration of the remaining 413 low-risk GC tissues and 624 high-risk GC tissues (Fig. 10a). The high-risk GC tissues exhibited a lower infiltration level of T cells follicular helper, T cells memory activated, and Macrophage M0, but a higher infiltration level of T cells memory resting than the low-risk GC tissues (Fig. 10b). Coincidentally, it was found that the higher infiltration level of T cells memory resting was not conducive to the prognosis of GC patients, while the higher infiltration level of Macrophage M0, T cells memory activated, and T cells follicular helper showed an opposite result (Fig. 10c). Therefore, the different clinical outcomes of GC patients may be related to tumor immunity.

Clinical correlation analysis for the risk score

The stage T, stage N, stage M, and stage TNM were closely related to the prognosis of GC patients, and the patients's risk score were positively correlated with the stage T, stage N, stage M, and stage TNM (Fig. 11a–e). The patients with lauren classification's diffuse and mixed type had poorer prognosis and higher risk score. However, there was no significant correlation between tumor grade and prognosis (Fig. 11f).

The prognostic signature's underlying molecular mechanism

We identified the differential expressed genes (DEGs) in different risk groups using the R package "limma"(fdrFilter = 0.05, logFCfilter = 1) (Fig. 12a). Among 996 DEGs, 929 genes were up-regulated in high-risk group and 67 genes were down-regulated (Additional file 2). We conducted Gene Ontology (GO) annotation and KEGG pathway enrichment analysis for the DEGs up-regulated in the high-risk group with the R package "clusterProfiler", and found that the GO terms related to extracellular structure organization and extracellular matrix organization were associated with high-risk group (Fig. 12b). The activity of calcium signaling pathway, cGMP-PKG signaling pathway, and PI3K-Akt signaling pathway were enhanced in the high-risk group (Fig. 12c). Besides, we also identified 9 gene sets positively correlated with the high-risk group by gene sets enrichment analysis (GSEA), such as the hallmark of angiogenesis, hypoxia, and epithelial-mesenchymal transition (EMT), etc.(Fig. 12d; Table 3), the "h.all.v7.1.symbols.gmt" were regarded as an reference.

Discussion

Gastric cancer (GC) is a typically malignant tumor of the digestive tract, since most GC patients were diagnosed in the advanced stage with a poor prognosis [24]. In recent years, comprehensive genomic research of GC has received growing attention [25], but the valuable biomarkers can be assisted in clinical diagnosis and treatment were still lacking [26]. The current methods of predicting prognosis cannot fully reflect the heterogeneity of GC, which usually difficult to accurately evaluate the clinical outcomes of GC [27]. Finding an precisely prognostic evaluation system could optimize the use of medical resources, which has important scientific and clinical significance [28].

Growing evidences have been suggested that the TP53 mutation can affect the immunophenotype of GC [13–15], but its mechanism still unclear. Maintaining genomic stability is one of the most important function of TP53. In the beginning of our study, we posed a hypothesis that the change of immune genome expression pattern mediated by TP53 mutation may affect the immunophenotype of GC and lead to different clinical outcomes. As expected, we found different infiltration levels of several immune cells in the GC tissues with and without TP53 mutation, as well as the expression levels of immune-related genes. There are few reports about the effect of

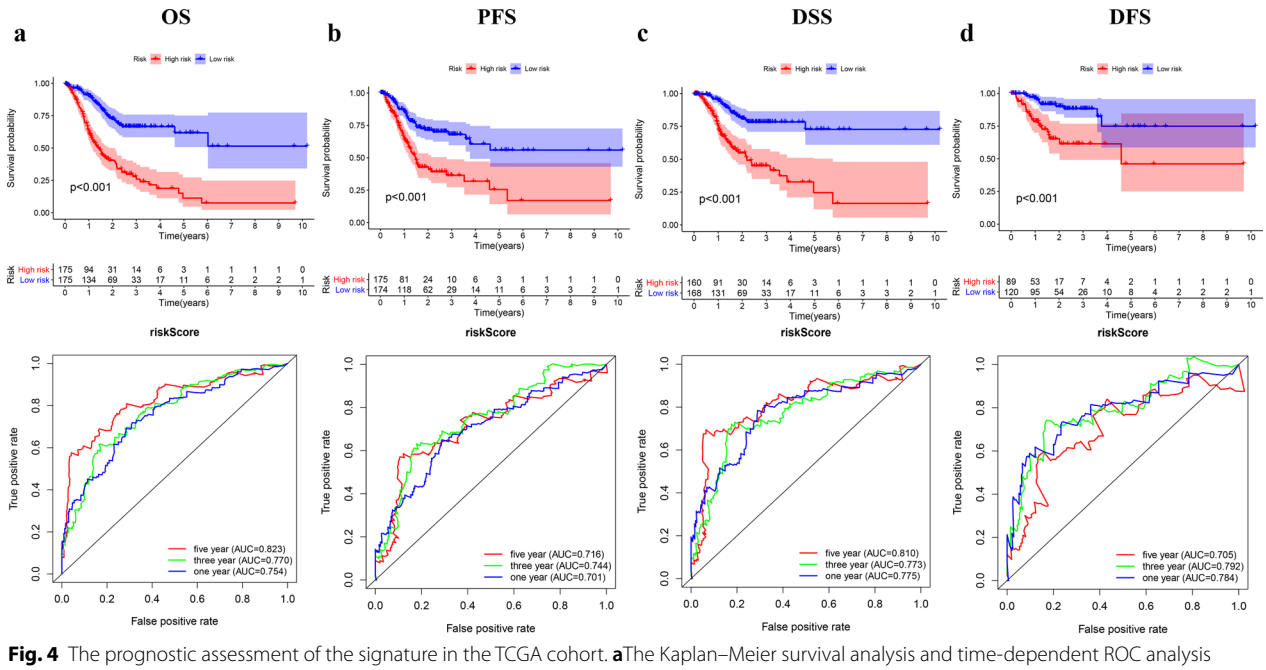

Fig. 4 The prognostic assessment of the signature in the TCGA cohort. **a**The Kaplan–Meier survival analysis and time-dependent ROC analysis of the signature for predicting the OS of patients in the TCGA cohort. **b** The Kaplan–Meier survival analysis and time-dependent ROC analysis of the signature for predicting the PFS of patients in the TCGA cohort. **c** The Kaplan–Meier survival analysis and time-dependent ROC analysis of the signature for predicting the DSS of patients in the TCGA cohort. **d** The Kaplan–Meier survival analysis and time-dependent ROC analysis of the signature for predicting the DFS of patients in the TCGA cohort

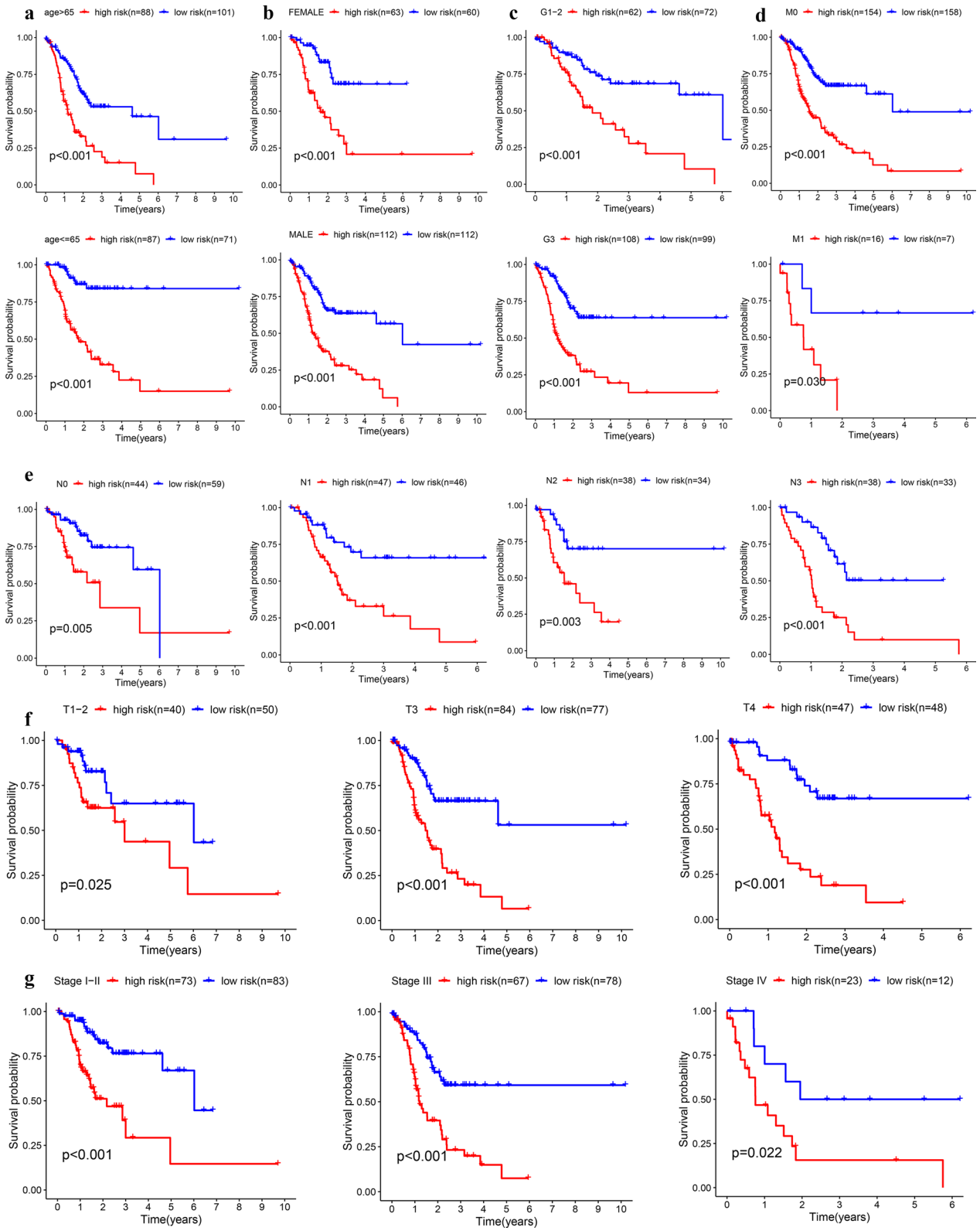

Fig. 5 Subgroup survival analysis based on clinical features for internal validation. **a** Age, **b** Gender, **c** Grade, **d** stage M, **e** stage N, **f** stage T, **g** stage TNM

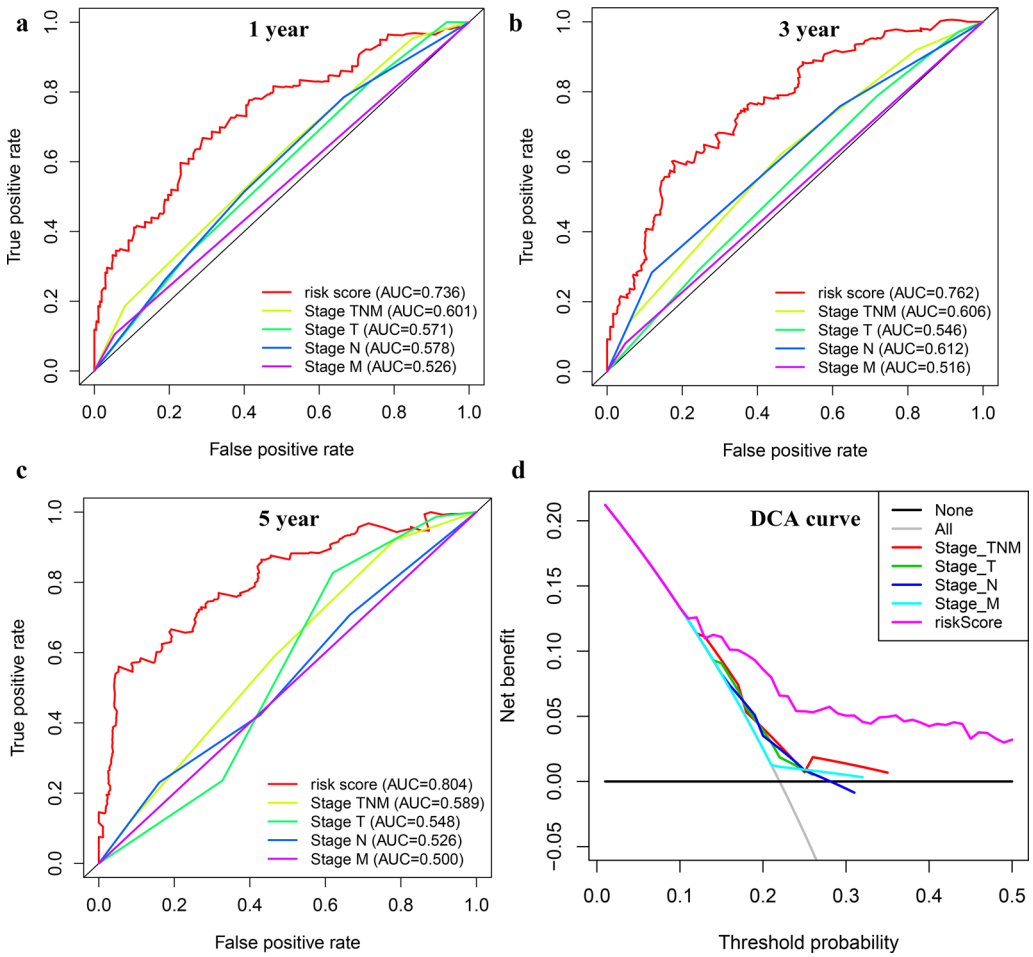

Fig. 6 Comparison of the prognostic model and TNM stage system. **a** 1-year time-dependent ROC curve, **b** 3-year time-dependent ROC curve, **c** 5-year time-dependent ROC curve, **d** DCA curve

this difference on the prognosis of GC so far. Next, we focused on the construction and validation of the prognosis model according to this clue, for improving the currently used prognosis evaluation system.

Considering the units of gene expression were not standardized, the traditional prognostic signature based on gene expression levels with limited applicability for the assessment of the prognosis of GC [29]. Developing a new prognostic model with universal applicability has become an urgent need in the research field of GC. Since the gene pairs were generated by a pairwise comparison based on the gene expression in the same patient, the gene expression profiles of different platforms did not need to be normalized [30], which made this method more convenient to use.

A total of 11 immune gene pairs were screened out to construct a risk score through multivariate Cox regression analysis, Lasso regression and univariate Cox analysis. In the TCGA cohort, the prognostic model showed good predictive performance for OS, PFS, DSS, and DFS of GC patients. To further evaluate the models' applicability, we carried out subgroup analysis and external validation. The results of subgroup analysis showed that the model was suitable for GC patients with different characteristics. It is worth mentioning that our model could capable of distinguish between GC patients with good prognosis and poor prognosis in all four independent external validation cohort. Besides, the risk score was identified to be an independent prognostic indicator in each independent cohort. These evidences indicated that the prognostic model has great potential for clinical application. Another important finding is the two groups' significant difference in the proportion of immune cell infiltration, which could be explained by the prognosis of GC patients. This finding demonstrated that we could evaluate the immune response of GC tissue according to the prognostic model, which has important guiding significance for the development

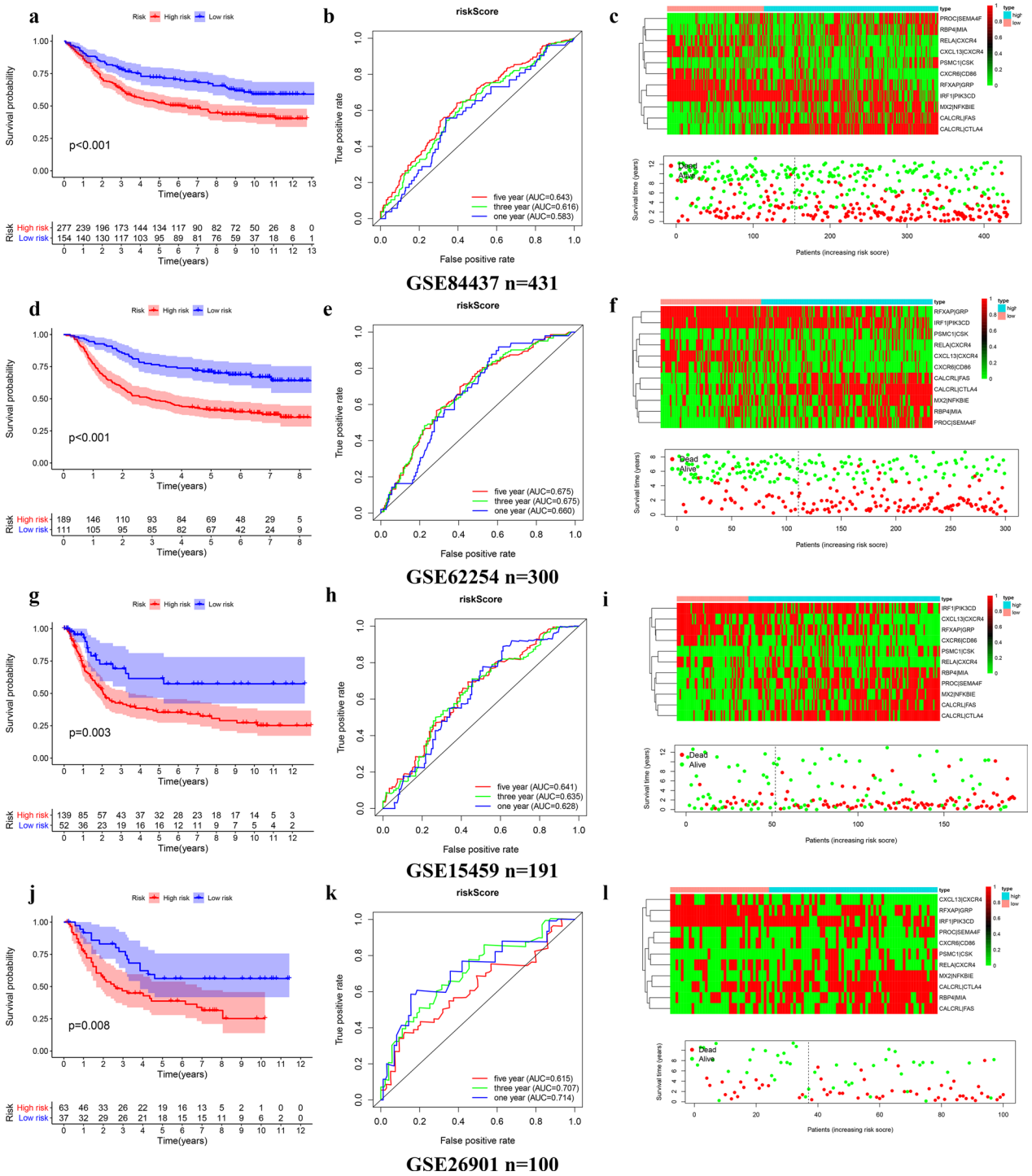

Fig. 7 The Kaplan–Meier survival analysis, time-dependent ROC analysis, and the heatmap, survival status of patients in four independent external validation cohorts, **a**–**c** GSE84437 cohort, **d**–**f** GSE62254 cohort, **g**–**i** GSE15459 cohort, **j**–**l** GSE26901 cohort

of individualized treatment plan for GC patients. We also compared it with the TP53 associated 9 immune gene signature constructed by Nie et al. [29]. The AUC values for Nie's TP53 associated 9 immune gene signature predicting OS at 1,3 and 5 years were 0.691,0.704 and 0.742 respectively, while the AUC values for our

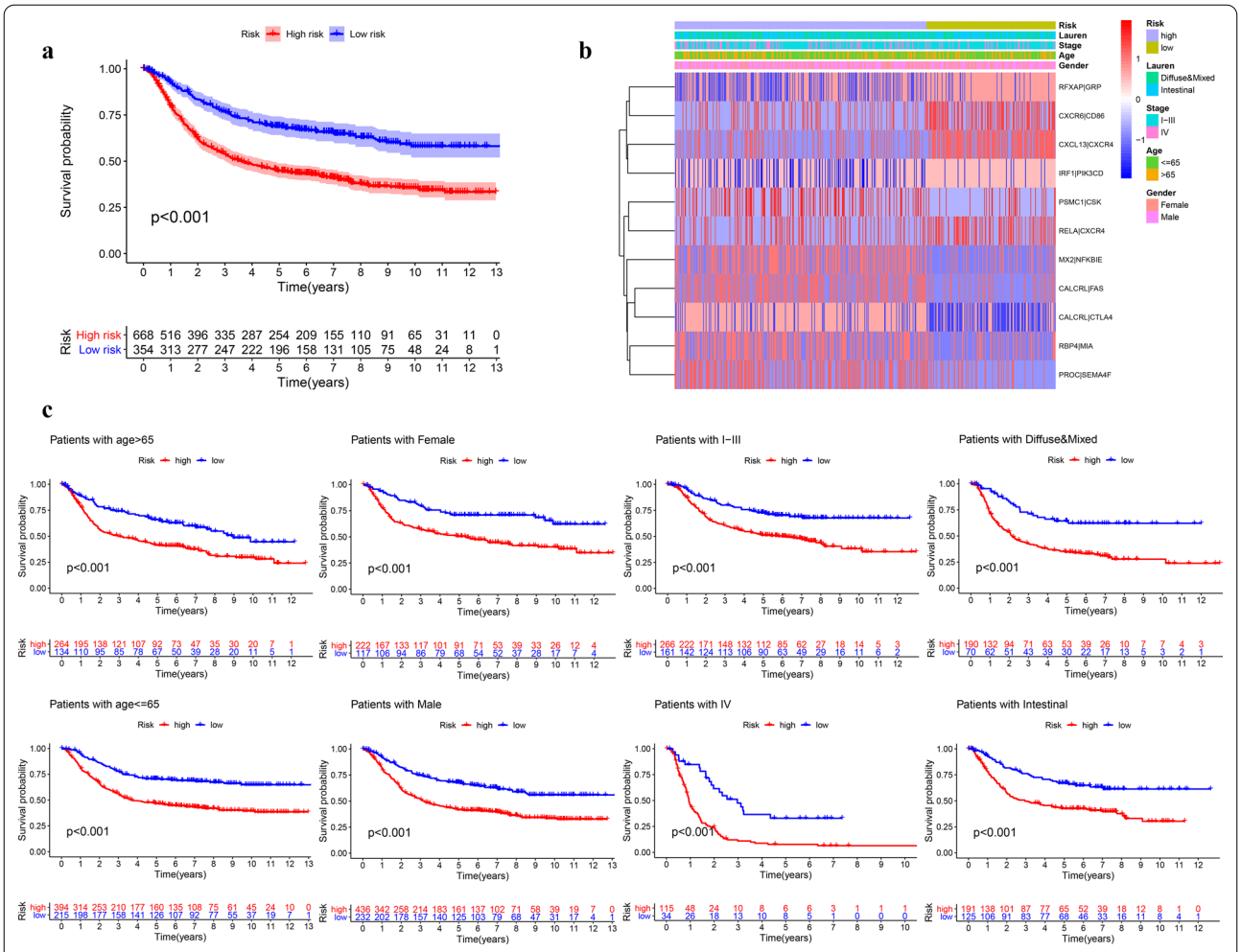

Fig. 8 The Prognostic assessment of the signature in the entire-external validation samples. **a** The Kaplan–Meier survival analysis, **b** Heatmap, **c** clinical grouping validation

model predicting OS at 1,3 and 5 years were0.754,0.770 and 0.823 respectively, which confirmed the superiority of the model further.

In order to reveal the potential reasons for the difference of prognosis between high-risk group and low-risk group, we observed the distribution of risk score in GC patients with different clinical characteristics. Although there was no significant correlation between risk score and tumor differentiation, risk score was positively correlated with the stage T, stage N, stage M, and stage TNM, and the risk score of patients with lauren classification's diffuse and mixed type were also significantly higher than patients with lauren classification's intestinal type. These results suggested that we can predict the degree of tumor invasion, lymph node metastasis and pathological classification according to the risk score. GO annotation showed that the terms related to extracellular structure organization and extracellular matrix organization were up-regulated in the high-risk group, which indicated that the polarity and skeleton structure of GC cells in

(See figure on next page.)

Fig. 9 Independence validation of the prognostic signature in the 5 independent cohort. **a** The forrest plot of the univariate and multivariate Cox analysis in TCGA. **b** The forrest plot of the univariate and multivariate Cox analysis in GSE84437. **c** The forrest plot of the univariate and multivariate Cox analysis in GSE62254. **d** The forrest plot of the univariate and multivariate Cox analysis in GSE15459. **e** The forrest plot of the univariate and multivariate Cox analysis in GSE26901. *Green represents univariate analysis, and red represents multivariate analysis

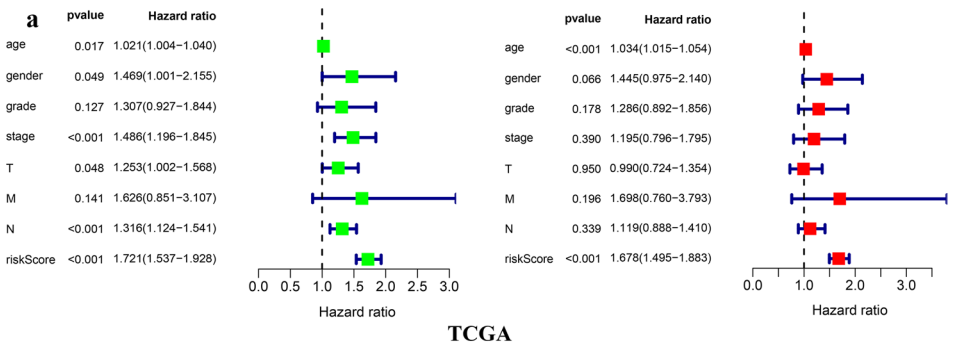
a
pvalue
Hazard ratio
age 0.017 1.021(1.004−1.040)
gender 0.049 1.469(1.001−2.155)
grade 0.127 1.307(0.927−1.844)
stage <0.001 1.486(1.196−1.845)
T 0.048 1.253(1.002−1.568)
M 0.141 1.626(0.851−3.107)
N <0.001 1.316(1.124−1.541)
riskScore <0.001 1.721(1.537−1.928)
0.0 0.5 1.0 1.5 2.0 2.5 3.0
Hazard ratio
pvalue
Hazard ratio
age <0.001 1.034(1.015−1.054)
gender 0.066 1.445(0.975−2.140)
grade 0.178 1.286(0.892−1.856)
stage 0.390 1.195(0.796−1.795)
T 0.950 0.990(0.724−1.354)
M 0.196 1.698(0.760−3.793)
N 0.339 1.119(0.888−1.410)
riskScore <0.001 1.678(1.495−1.883)
0.0 1.0 2.0 3.0
Hazard ratio
TCGA

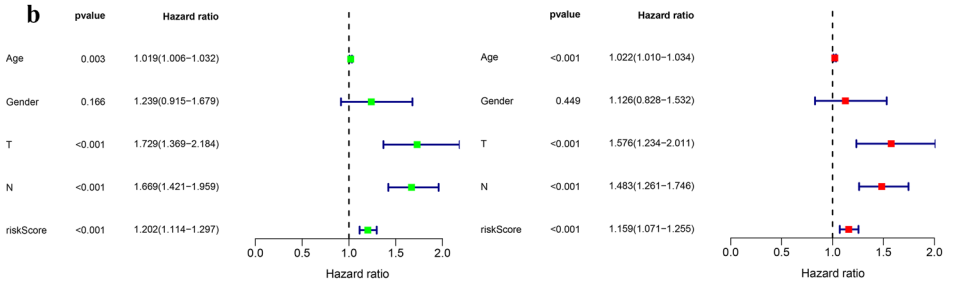
b
pvalue
Hazard ratio
Age 0.003 1.019(1.006−1.032)
Gender 0.166 1.239(0.915−1.679)
T <0.001 1.729(1.369−2.184)
N <0.001 1.669(1.421−1.959)
riskScore <0.001 1.202(1.114−1.297)
0.0 0.5 1.0 1.5 2.0
Hazard ratio
pvalue
Hazard ratio
Age <0.001 1.022(1.010−1.034)
Gender 0.449 1.126(0.828−1.532)
T <0.001 1.576(1.234−2.011)
N <0.001 1.483(1.261−1.746)
riskScore <0.001 1.159(1.071−1.255)
0.0 0.5 1.0 1.5 2.0
Hazard ratio
GSE84437

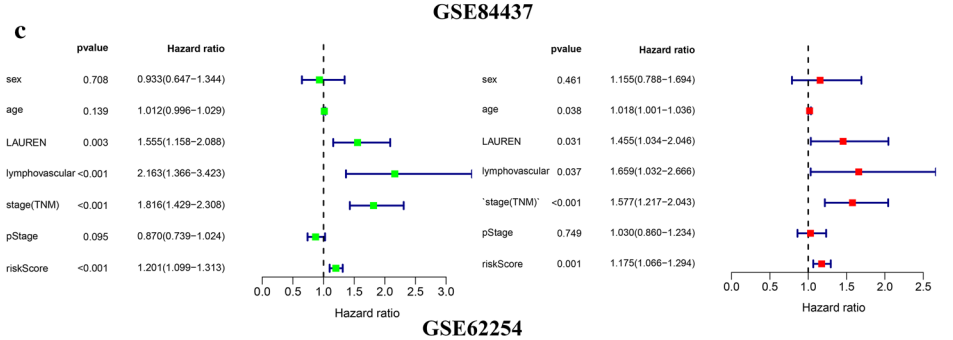
c
pvalue
Hazard ratio
sex 0.708 0.933(0.647−1.344)
age 0.139 1.012(0.996−1.029)
LAUREN 0.003 1.555(1.158−2.088)
lymphovascular <0.001 2.163(1.366−3.423)
stage(TNM) <0.001 1.816(1.429−2.308)
pStage 0.095 0.870(0.739−1.024)
riskScore <0.001 1.201(1.099−1.313)
0.0 0.5 1.0 1.5 2.0 2.5 3.0
Hazard ratio
pvalue
Hazard ratio
sex 0.461 1.155(0.788−1.694)
age 0.038 1.018(1.001−1.036)
LAUREN 0.031 1.455(1.034−2.046)
lymphovascular 0.037 1.659(1.032−2.666)
`stage(TNM)` <0.001 1.577(1.217−2.043)
pStage 0.749 1.030(0.860−1.234)
riskScore 0.001 1.175(1.066−1.294)
0.0 0.5 1.0 1.5 2.0 2.5
Hazard ratio
GSE62254

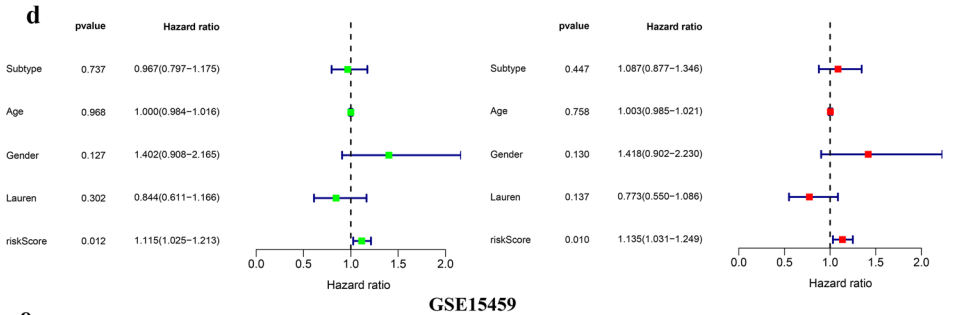
d
pvalue
Hazard ratio
Subtype 0.737 0.967(0.797−1.175)
Age 0.968 1.000(0.984−1.016)
Gender 0.127 1.402(0.908−2.165)
Lauren 0.302 0.844(0.611−1.166)
riskScore 0.012 1.115(1.025−1.213)
0.0 0.5 1.0 1.5 2.0
Hazard ratio
pvalue
Hazard ratio
Subtype 0.447 1.087(0.877−1.346)
Age 0.758 1.003(0.985−1.021)
Gender 0.130 1.418(0.902−2.230)
Lauren 0.137 0.773(0.550−1.086)
riskScore 0.010 1.135(1.031−1.249)
0.0 0.5 1.0 1.5 2.0
Hazard ratio
GSE15459

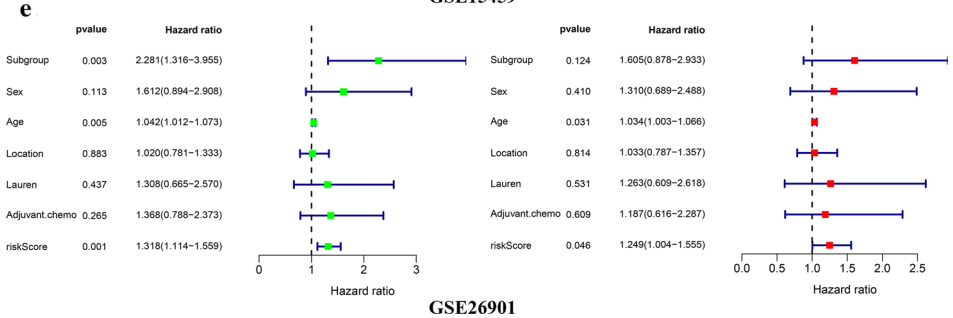
e
pvalue
Hazard ratio
Subgroup 0.003 2.281(1.316−3.955)
Sex 0.113 1.612(0.894−2.908)
Age 0.005 1.042(1.012−1.073)
Location 0.883 1.020(0.781−1.333)
Lauren 0.437 1.308(0.665−2.570)
Adjuvant.chemo 0.265 1.368(0.788−2.373)
riskScore 0.001 1.318(1.114−1.559)
0 1 2 3
Hazard ratio
pvalue
Hazard ratio
Subgroup 0.124 1.605(0.878−2.933)
Sex 0.410 1.310(0.689−2.488)
Age 0.031 1.034(1.003−1.066)
Location 0.814 1.033(0.787−1.357)
Lauren 0.531 1.263(0.609−2.618)
Adjuvant.chemo 0.609 1.187(0.616−2.287)
riskScore 0.046 1.249(1.004−1.555)
0.0 0.5 1.0 1.5 2.0 2.5
Hazard ratio
GSE26901

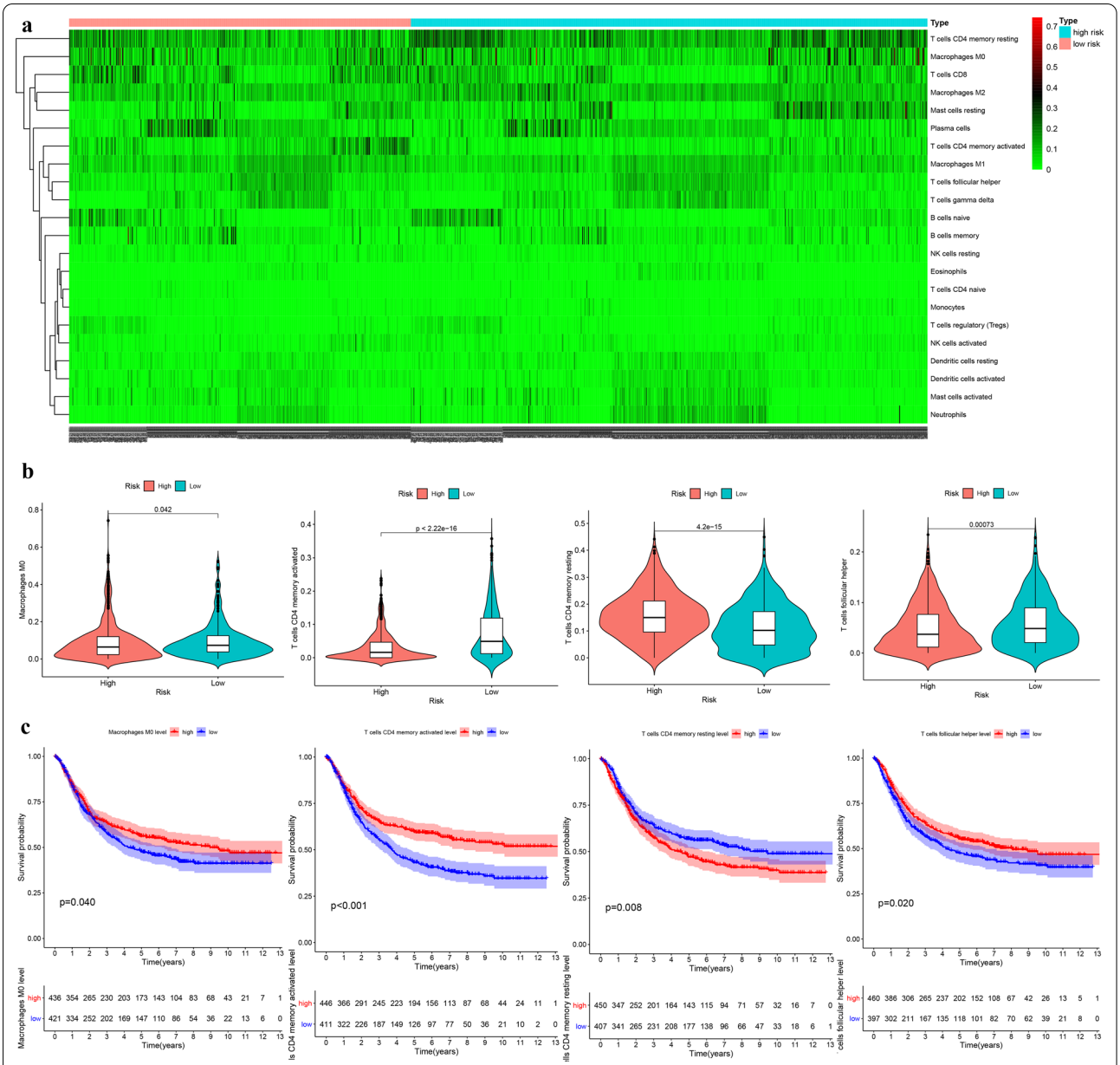

Fig. 10 The difference of immune cell infiltration between high- and low-risk groups. **a** The heatmap of immune infiltration landscape. **b** The vioplot of the difference of the infiltration level of the T cells memory activated, T cells memory resting, T cells follicular helper, and Macrophage M0 between high- and low-risk groups. **c** The Kaplan–Meier survival analysis of the infiltration level of the T cells memory activated, T cells memory resting, T cells follicular helper, and Macrophage M0

high-risk group are more likely to change, thus showing high invasiveness [31]. KEGG pathway enrichment analysis demonstrated that the risk score may stimulated the proliferation of GC cells by activating the PI3K-Akt signaling pathway [32], which consistent with the presentation of GSEA's results suggested that the expression of angiogenesis and hypoxia related gene sets were up-regulated in the high-risk group. Because the continuous proliferation of tumor cells needs angiogenesis to provide nutrients, in the process of GC tumor proliferation, the increase of the distance between tumor cells and the surrounding stromal vessels will lead to hypoxia in the tumor [33]. In addition, the EMT related gene sets were also up-regulated in the high-risk group, indicated that the patients with higher risk score were prone to invasion and metastasis [34].

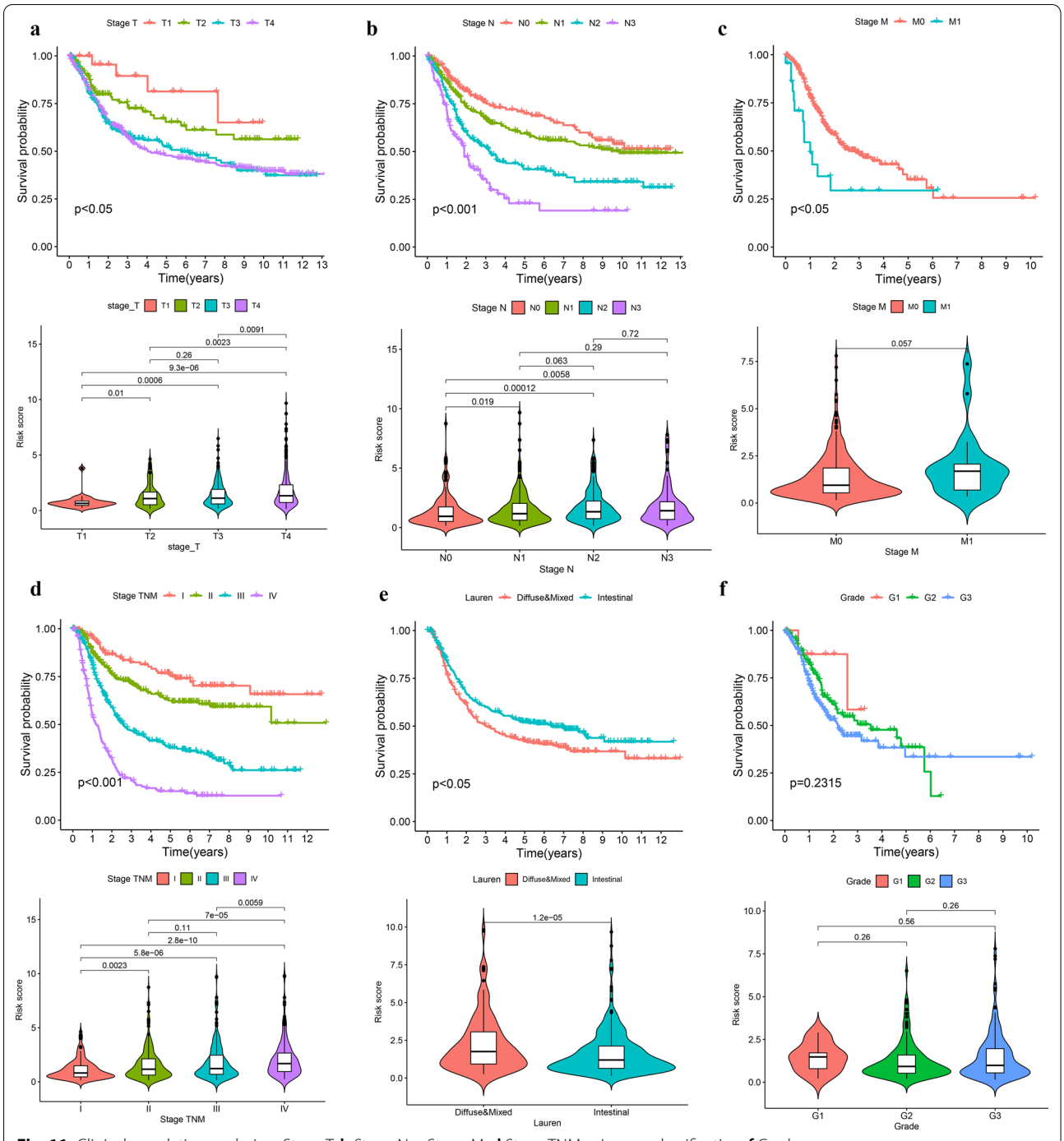

Fig. 11 Clinical correlation analysis. **a** Stage T. **b** Stage N. **c** Stage M. **d** Stage TNM. **e** Lauren classification. **f** Grade

A few of genes in the model have been confirmed to play a role in the occurrence and progression of GC. For example, Izumi [35] reported that the stimulation of CXCR4 promoted the invasive ability of GC cells. Liu [36] found that the PIK3CD was a core oncogene involved in the progression of GC. Yamaguchi [37] demonstrated that the macrophages M2 (CD86(+)) could contribute to the proliferation and progression of GC. Wang [38] demonstrated the correlation of the downregulation of FAS expression with increased lymph node and distant metastases of GC as well as less histological differentiation and gender (male). Wei

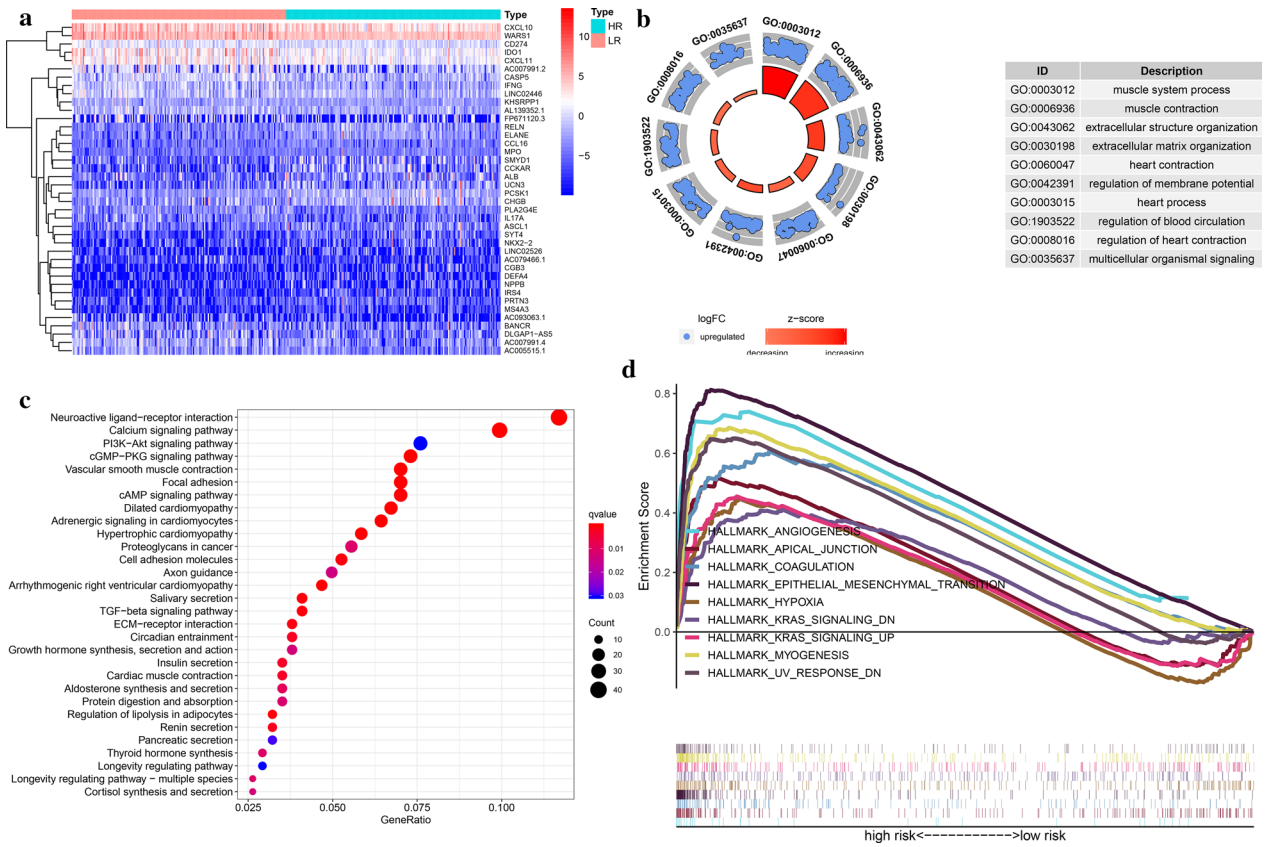

Fig. 12 The prognostic model's underlying molecular mechanism. **a** The heatmap of DEGs between high- and low-risk groups. **b** The GO annotation of the DEGs up-regulated in the high-risk group. **c** The KEGG pathway enrichment analysis for the DEGs up-regulated in the high-risk group. **d** The 9 gene sets identified by GSEA positively correlated with the high-risk group

Table 3 The 9 gene sets identified by GSEA showed positive correlation with the high-risk group

Name	ES	NES	NOM p-val	FDR q-val	FWER p-val
HALLMARK_MYOGENESIS	0.685	2.302	0	0	0
HALLMARK_EPITHELIAL_MESENCHYMAL_TRANSITION	0.812	2.261	0	0.001	0.005
HALLMARK_ANGIOGENESIS	0.739	2.017	0	0.008	0.032
HALLMARK_COAGULATION	0.608	1.973	0	0.0103	0.048
HALLMARK_KRAS_SIGNALING_DN	0.412	1.652	0.004	0.081	0.276
HALLMARK_UV_RESPONSE_DN	0.650	2.042	0.004	0.008	0.025
HALLMARK_APICAL_JUNCTION	0.515	1.815	0.017	0.035	0.146
HALLMARK_KRAS_SIGNALING_UP	0.455	1.609	0.037	0.091	0.323
HALLMARK_HYPOXIA	0.448	1.545	0.046	0.098	0.399

[39] demonstrated the correlations of the high CXCL13 expression with lower OS and larger tumor diameter in GC.Yuan [40] supported the role of IRF-1 in hindering GC metastasis, which was achieved through the reduction of Wnt/β-catenin signaling and the downregulation of MIR17HG-miR-18a/miR-19a axis expression. Jin [41] identified CXCR6 to be an independent prognostic factor for poor survival in GC patients, which may played a role in advancing GC metastasis by means of epithelial-mesenchymal transition. Xiang [42] demonstrated that the activation of CXCR4 could promote the metastasis of GC. As there are few studies on the

remaining moleculars in GC and even cancers, their specific biological effects are still unclear. However, with the gradual deepening of the understanding of these new biomarkers, it will effectively promote the development of individualized and precise treatment for GC.

To sum up, this study was a retrospective study with large sample and multi centers. A total of 1372 GC patients from 5 independent cohort included in our work. We constructed and validated a valuable system to evaluate the prognosis of GC. Considering the stability and general applicability of the model, it may become a widely used tool in clinical practice. However, there are still some deficiencies in this study. First, although the overall effect of external validation in GEO database was satisfactory, the accuracy of the model in GEO external validation cohorts was not as good as TCGA cohort. Second, the gene pairs were generated by a pairwise comparison had important prognostic value for GC found by our work, but its underlying mechanism was not fully revealed by our paper, which needs further study. Third, our study was still a retrospective study and cannot replace a prospective multicenter clinical trials.

Conclusion

Our study proposed a novel system for evaluating the prognosis of gastric cancer. Considering its stability and general applicability, which may become a widely used tool in clinical practice.

Abbreviations

GC: Gastric cancer; TCGA: The Cancer Genome Atlas; GEO: Gene Expression Ominibus; DEIRGs: Differential expressed immune-related genes; DEGs: Differential expressed genes; KEGG: Kyoto Encyclopedia of Genes and Genomes; GO: Gene Ontology; GSEA: Gene Sets Enrichment Analysis; EMT: Epithelial-mesenchymal transition; TNM: Tumor Lymph Node Metastasis; TIMER: Tumor IMmune Estimation Resource; GPs: Gene pairs; IGP: Immune gene pair; PRIGPs: Prognostic related immune gene pairs; ROC: Receiver operating characteristic; AUC: Area under curve; OS: Overall survival; DSS: Disease special survival; DFS: Disease free survival; PFS: Progression free survival; RFS: Recurrent free survival.

Supplementary Information

The online version contains supplementary material available at https://doi.org/10.1186/s12967-021-02846-x.

Additional file 1: The immune related gene list obtained from the ImmPort database.

Additional file 2: The differential expressed genes in different risk groups.

Additional file 3: The timedependent ROC curve for the signature predicting OS of meta-GEO cohort (1022 patients).

Additional file 4: Source code (https://github.com/huojunyu/JTRM-D-21-00055).

Acknowledgements

None

Authors' contributions

JH and LW designed this study, JH analyzed the data in this study and interpreted the findings and drafted the manuscript. JH, LW and YZ carried out data management and revised the manuscript. All authors reviewed the final version of the manuscript.

Funding

None.

Availability of data and materials

The datasets analysed for this study were obtained from The Cancer Genome Atlas (TCGA)(https://portal.gdc.cancer.gov/), the cBioPortal (https://www.cbioportal.org/) and Gene Expression Omnibus (GEO) (https://www.ncbi.nlm.nih.gov/geo/).

Declaration

Ethics approval and consent to participate

Not applicable.

Consent for publication

The manuscript is approved by all authors for publication.

Competing interests

The authors have no conflicts of interest to declare.

Author details

[1]Liver Disease Center, The Affiliated Hospital of Qingdao University, No. 59 Haier Road, Qingdao 266003, China. [2]Qingdao University, No. 308 Ningxia Road, Qingdao 266071, China.

Received: 10 January 2021 Accepted: 18 April 2021
Published online: 29 April 2021

References

1. Sexton RE, Al Hallak MN, Diab M, Azmi AS. Gastric cancer: a comprehensive review of current and future treatment strategies. Cancer Metastasis Rev 2020:1–25.
2. Y Kurokawa H-K Yang H Cho M-H Ryu T Masuzawa SR Park S Matsumoto H-J Lee H Honda 2017 Kwon OKJBjoc: Phase II study of neoadjuvant imatinib in large gastrointestinal stromal tumours of the stomach Br J Cancer 117 1 25 32
3. LA Donehower T Soussi A Korkut Y Liu A Schultz M Cardenas X Li O Babur TK Hsu O Lichtarge 2019 Integrated analysis of TP53 gene and pathway alterations in the cancer genome atlas Cell Rep 28 5 1370 1384 e1375
4. MB Kastan CE Canman CJ Leonard 1995 P53, cell cycle control and apoptosis: implications for cancer Cancer Metastais Rev 14 1 3 15
5. C Kandoth MD McLellan F Vandin K Ye B Niu C Lu M Xie Q Zhang JF McMichael MAJN Wyczalkowski 2013 Mutational landscape and significance across 12 major cancer types Nature 502 7471 333 339
6. S Park J Lee YH Kim J Park J-W Shin S Nam 2016 Clinical relevance and molecular phenotypes in gastric cancer, of TP53 mutations and gene expressions, in combination with other gene mutations Sci Rep 6 34822
7. Y Zha P Gan Q Liu Q Yao 2016 TP53 codon 72 polymorphism predicts efficacy of paclitaxel plus capecitabine chemotherapy in advanced gastric cancer patients Arch Med Res 47 1 13 18
8. Z-Y Dong W-Z Zhong X-C Zhang J Su Z Xie S-Y Liu H-Y Tu H-J Chen Y-L Sun Q Zhou 2017 Potential predictive value of TP53 and KRAS mutation status for response to PD-1 blockade immunotherapy in lung adenocarcinoma Clin Cancer Res 23 12 3012 3024
9. J Biton A Mansuet-Lupo N Pécuchet M Alifano H Ouakrim J Arrondeau P Boudou-Rouquette F Goldwasser K Leroy J Goc 2018 TP53, STK11, and EGFR mutations predict tumor immune profile and the response to anti–PD-1 in lung adenocarcinoma Clin Cancer Res 24 22 5710 5723

10. D Menendez A Inga 2009 Resnick MAJNrC: The expanding universe of p53 targets Nat Rev Cancer 9 10 724 737
11. Y Cui G Guo 2016 Immunomodulatory function of the tumor suppressor p53 in host immune response and the tumor microenvironment Int J Mol Sci 17 11 1942
12. S Matsueda DY Graham 2014 Immunotherapy in gastric cancer World J Gastroenterol 20 7 1657
13. Z Jiang Z Liu M Li C Chen X Wang 2018 Immunogenomics analysis reveals that TP53 mutations inhibit tumor immunity in gastric Cancer Transl Oncol 11 5 1171 1187
14. C Muñoz-Fontela A Mandinova SA Aaronson 2016 Lee SW Emerging roles of p53 and other tumour-suppressor genes in immune regulation Nat Rev Immunol 16 12 741 750
15. KW Yoon S Byun E Kwon S-Y Hwang K Chu M Hiraki S-H Jo A Weins S Hakroush AJS Cebulla 2015 Control of signaling-mediated clearance of apoptotic cells by the tumor suppressor Science 349 6247 53
16. J Huo L Wu Y Zang 2021 Medicine M: development and validation of a CTNNB1-associated metabolic prognostic model for hepatocellular carcinoma J Cell Mol Med 25 2 1151 1165
17. J Huo L Wu Y Zang 2020 A prognostic model of 15 immune-related gene pairs associated with tumor mutation burden for hepatocellular carcinoma Front mol Biosci https://doi.org/10.3389/fmolb.2020.581354
18. AM Newman CL Liu MR Green AJ Gentles W Feng Y Xu CD Hoang M Diehn AA Alizadeh 2015 Robust enumeration of cell subsets from tissue expression profiles Nat Methods 12 5 453 457
19. J Huo L Wu Y Zang 2020 Development and validation of a novel immune-gene pairs prognostic model associated with CTNNB1 alteration in hepatocellular carcinoma Med Sci Monitor Int Med J Exp Clin Res 26 e925494 e925494
20. J Huo L Wu Y Zang H Dong X Liu F He X Zhang 2021 Eight-gene metabolic signature related with tumor-associated macrophages predicting overall survival for hepatocellular carcinoma BMC Cancer 21 1 1 15
21. T Li J Fan B Wang N Traugh Q Chen JS Liu B Li XS Liu 2017 TIMER: a web server for comprehensive analysis of tumor-infiltrating immune cells Cancer Res 77 21 e108 e110
22. B Li E Severson J-C Pignon H Zhao T Li J Novak P Jiang H Shen JC Aster S Rodig 2016 Comprehensive analyses of tumor immunity: implications for cancer immunotherapy Genome Biol 17 1 1 16
23. AJ Vickers EB Elkin 2006 Decision curve analysis: a novel method for evaluating prediction models Med Decis Making 26 6 565 574
24. AP Thrift HB El-Serag 2020 Hepatology: burden of gastric cancer Clin Gastroenterol Hepatol 18 3 534 542
25. JK Sa JY Hong I-K Lee J-S Kim M-H Sim HJ Kim JY An TS Sohn JH Lee JM Bae 2020 Comprehensive pharmacogenomic characterization of gastric cancer Genome Med 12 1 1 12
26. TH Patel M Cecchini 2020 Targeted therapies in advanced gastric cancer Curr Treat Options Oncol 21 9 1 14
27. T Sano DG Coit HH Kim F Roviello P Kassab C Wittekind Y Yamamoto Y Ohasi 2017 Proposal of a new stage grouping of gastric cancer for TNM classification: International Gastric Cancer Association staging project Gastric Cancer 20 2 217 225
28. LH Eusebi A Telese G Marasco F Bazzoli RM Zagari 2020 Hepatology: gastric cancer prevention strategies: a global perspective J Gatroenterol Hepatol 35 9 1495 1502
29. K Nie Z Zheng Y Wen L Shi S Xu X Wang Y Zhou B Fu X Li ZJG Deng 2020 Construction and validation of a TP53-associated immune prognostic model for gastric cancer Genomics 112 6 4788 4795
30. XY Sun SZ Yu HP Zhang J Li WZ Guo SJ Zhang 2020 A signature of 33 immune-related gene pairs predicts clinical outcome in hepatocellular carcinoma Cancer Med 9 8 2868 2878
31. C Walker E Mojares A Río Hernández Del 2018 Role of extracellular matrix in development and cancer progression Int J Mol Sci 19 10 3028
32. M Martini MC Santis De L Braccini F Gulluni E Hirsch 2014 PI3K/AKT signaling pathway and cancer: an updated review Ann Med. 46 6 372 383
33. O Stoeltzing MF McCarty JS Wey F Fan W Liu A Belcheva CD Bucana GL Semenza LM Ellis 2004 Role of hypoxia-inducible factor 1α in gastric cancer cell growth, angiogenesis, and vessel maturation J Natl Cancer Inst 96 12 946 956
34. L Huang R-L Wu A-M Xu 2015 Epithelial-mesenchymal transition in gastric cancer Am J Tansl Res 7 11 2141
35. D Izumi T Ishimoto K Miyake H Sugihara K Eto H Sawayama T Yasuda Y Kiyozumi T Kaida J Kurashige 2016 CXCL12/CXCR4 activation by cancer-associated fibroblasts promotes integrin β1 clustering and invasiveness in gastric cancer Int J Cancer 138 5 1207 1219
36. Liu H-T, Ma R-R, Lv B-B, Zhang H, Shi D-B, Guo X-Y, Zhang G-H, Gao P. LncRNA-HNF1A-AS1 functions as a competing endogenous RNA to activate PI3K/AKT signalling pathway by sponging miR-30b-3p in gastric cancer. Br J Cancer 2020:1–12.
37. T Yamaguchi S Fushida Y Yamamoto T Tsukada J Kinoshita K Oyama T Miyashita H Tajima I Ninomiya S Munesue 2016 Tumor-associated macrophages of the M2 phenotype contribute to progression in gastric cancer with peritoneal dissemination Gastric Cancer 19 4 1052 1065
38. X Wang Z Fu Y Chen L Liu 2017 Fas expression is downregulated in gastric cancer Mol Med Rep 15 2 627 634
39. Y Wei C Lin H Li Z Xu J Wang R Li H Liu H Zhang H He J Xu 2018 Immunotherapy: CXCL13 expression is prognostic and predictive for postoperative adjuvant chemotherapy benefit in patients with gastric cancer Cancer Immunol Immunother 67 2 261 269
40. J Yuan L Tan Z Yin W Zhu K Tao G Wang W Shi J Gao 2019 MIR17HG-miR-18a/19a axis, regulated by interferon regulatory factor-1, promotes gastric cancer metastasis via Wnt/β-catenin signalling Cell Death Dis 10 6 1 16
41. J-J Jin F-X Dai Z-W Long H Cai X-W Liu Y Zhou Q Hong Q-Z Dong Y-N Wang H Huang 2017 CXCR6 predicts poor prognosis in gastric cancer and promotes tumor metastasis through epithelial-mesenchymal transition Oncol Rep 37 6 3279 3286
42. Z Xiang Z Zhou G Xia X Zhang Z Wei J Zhu J Yu W Chen Y He RJ Schwarz 2017 A positive crosstalk between CXCR4 and CXCR2 promotes gastric cancer metastasis Oncogene 36 36 5122 5133

Publisher's Note

Springer Nature remains neutral with regard to jurisdictional claims in published maps and institutional affiliations.

Ready to submit your research? Choose BMC and benefit from:

- fast, convenient online submission
- thorough peer review by experienced researchers in your field
- rapid publication on acceptance
- support for research data, including large and complex data types
- gold Open Access which fosters wider collaboration and increased citations
- maximum visibility for your research: over 100M website views per year

At BMC, research is always in progress.

Learn more biomedcentral.com/submissions

BMC